

Theoretical electronic properties of TiO₂ (rutile) (001) and (110) surfaces

R. V. Kasowski and R. H. Tait

Central Research and Development Department, E. I. du Pont de Nemours and Company, Wilmington, Delaware 19898

(Received 18 June 1979)

We have calculated the one-electron density of states of thick slabs of TiO₂ (rutile) with (001) and (110) symmetry using the linear combination of muffin-tin orbitals (LCMTO) energy-band method. We have also calculated the density of states of bulk TiO₂ and of bulk Ti₂O₃. We found that the local titanium-oxygen coordination is the major factor determining the band structures of these surface and bulk systems. In particular, for the unreconstructed (001) face of TiO₂, we found that there is a large band of occupied surface states in the bulk band gap while there are no occupied states for the unreconstructed (but slightly relaxed) (110) surface. Our results suggest that the (001) face reconstructs to increase the local coordination of titanium in order to eliminate these band-gap surface states.

I. INTRODUCTION

The properties of single-crystal surfaces of TiO₂ (rutile) have been measured experimentally by a variety of methods including photoelectrolysis,^{1,2} ultraviolet photoelectron spectroscopy (UPS),³⁻⁵ low-energy-electron diffraction (LEED)³⁻⁵ and electron-energy-loss spectroscopy (ELS).^{3,4} However, comparable theoretical surface studies of TiO₂ have not been previously reported. We present here the first *ab initio* theoretical investigation of the surface properties of TiO₂. The linear combination of muffin-tin orbitals (LCMTO) energy-band method^{6,7} was employed to calculate *ab initio* energy bands for thin films (three to five layers thick) of TiO₂ with (110) or (001) symmetry as well as for bulk TiO₂ and bulk Ti₂O₃. Our aims in this study were to: (1) investigate the role played by local atomic coordination in determining both the surface and bulk one-electron density of states (DOS) for TiO₂ and (2) examine the role of surface band structure in determining the surface stability of this material.

The (001) and (110) faces were selected for examination because they exhibit extremes in local atomic coordination, observed surface stability and calculated surface band structure. The (110) face (which has fivefold and sixfold oxygen-coordinated titanium atoms) is found to have the (1 × 1) LEED pattern of an unreconstructed surface,³⁻⁵ while the (001) face (which has only fourfold oxygen-coordinated titanium atoms) either facets⁴ and/or reconstructs⁵ after annealing. Our calculations show that for both faces there is a filled O(2*p*)-derived surface state band in the bulk band gap. However, our calculations show that for the stable (110) face⁸ this surface state band disappears completely into the bulk valence band when surface

O atoms are allowed to relax inward slightly. For the unstable (001) face, this filled O(2*p*) surface state band is quite large and cannot be removed by any simple relaxation. We conclude that these dangling-bond O(2*p*) surface states cause the unreconstructed (001) surface to be unstable and we conclude that this surface reconstructs to eliminate these unsaturated bonds.

Although *ab initio* bulk energy bands for TiO₂ have not been reported in the literature, empirically adjusted energy bands for TiO₂ have been calculated. Vos⁹ fitted an LCAO model to obtain an optical spectrum in good agreement with experiment. He predicted an indirect band gap to the *M* point for bulk TiO₂ in agreement with our results. Finally, Tossel *et al.*¹⁰ performed a scattered wave cluster calculation for TiO₂.

The only other comparable theoretical studies of surface properties of transition-metal oxides are the model calculations of Wolfram *et al.*¹¹ for (001) SrTiO₃. They also found bands of surface states in the band gap. These surface state bands were found to be very sensitive to the choice of Madelung potentials in agreement with our work. Wolfram *et al.* did not, however, investigate how the positions of the surface states are affected by surface atom relaxation.

In the remainder of this paper we will describe our calculations and discuss their implications. In Sec. II we describe the crystal structure of bulk TiO₂ and bulk Ti₂O₃. In Sec. II we also describe the structure of the (001) and (110) oriented films of TiO₂ used in this study. In Sec. III the details of the bulk and film DOS calculations are discussed. In Sec. IV we present the calculated band structures for the thin films of TiO₂ as well as for bulk TiO₂ and Ti₂O₃. Finally, in Sec. IV D we summarize our results.

II. CRYSTAL STRUCTURES—BULK AND FILMS

TiO_2 forms in the rutile structure shown in Fig. 1(a). This structure is tetragonal and contains six atoms in the unit cell. In the rutile structure each Ti atom is coordinated to six O atoms and each O atom is coordinated to three Ti atoms.

Ti_2O_3 forms in the α -alumina structure. This structure is hexagonal and has ten atoms per unit cell. In this structure each Ti atom is also coordinated to six O atoms but each O atom is coordinated to four Ti atoms.

For the (001) and (110) TiO_2 surface studies, a superlattice-crystal-structure model^{6,12} has been used. This model is constructed of thin films of TiO_2 separated by vacuum regions. (Since the vacuum spacing is chosen sufficiently large to eliminate interactions between TiO_2 films, the energy bands of this superlattice include the surface-energy bands). The (001) film [see Fig. 1(b)] is the simpler film to form. The (001) film contains three atoms per layer in its unit cell. A five layer TiO_2 (001) film (which contains 15 atoms in the film unit cell) was used in our calculations along with a three-layer vacuum spacing. The (110) film [see Fig. 1(c)] is more complex because the basic repeat layer is nonplanar and consists of six atoms in the unit cell. The (110) repeat layer actually consists of a central plane (two Ti atoms and two O atoms) with layers of O atoms lying 1.21 Å above and below the central plane. A three-layer TiO_2 (110) film (which con-

tains 18 atoms in the film unit cell), along with a two-layer vacuum region, was used in our calculations.

III. MTO BASIS SET AND POTENTIAL

The one-electron energy-band calculations discussed here were carried out using the LCMTO method.^{6,7,13-16} The energy bands of interest in our study are the valence bands and the conduction bands within a few eV of the gap. These bands extend over an energy range of about 13 eV (5-eV valence-band width, 3-eV gap, 5-eV d -band width). For the Ti atom, the optimal muffin-tin-orbital (MTO) basis set to describe these bands consists of sp^3d^5 MTO's with $\kappa^2=0.5$ Ry and $E=-0.7$ Ry. The optimal O basis set consists of two sets of sp^3 MTO's ($\kappa^2=0.5$ Ry and $E_1=-0.6$ Ry, $\kappa^2=-0.4$ Ry and $E_2=-1.0$ Ry). Therefore the number of basis functions for bulk rutile with six atoms per unit cell is 50 (i.e., 18 sp^3d^5 MTO's and 32 sp^3 MTO's). For a three-layer (110) film of TiO_2 the optimal number of basis functions would be 150 and for a five-layer (001) film the optimal number of basis functions would be 125. Our basis set is energy independent⁶ only if it contains adequate variational freedom so that only one diagonalization of the Hamiltonian is required per k point.

In the LCMTO energy-band method,⁶ the non-spherical part of the potential is included in the calculation. Because the crystal structures of TiO_2 and Ti_2O_3 are noncubic, 16 individual spherical harmonics are required within each atomic Wigner-Seitz cell to expand the potential to $l=6$. The computer time requirements rise very rapidly with the number of components in the potential and with the number of basis functions. As a result, a simplification in either the basis set or the potential was necessary to study TiO_2 films economically.

We decided to keep all 16 components of the potential but to reduce the number of basis functions. An MTO basis set with $\kappa^2=-0.4$ Ry was used on both the Ti and O atoms. Furthermore, only the s and d^5 MTO's were included on the Ti site. It is reasonable to ignore the Ti p^3 MTO's as they represent the Ti $4p$ states that are at least 7 eV above the conduction-band edge. These assumptions greatly reduce the number of basis functions which now becomes 28 for bulk TiO_2 (12 sd^5 MTO's and 16 sp^3 MTO's), 84 for a (110) TiO_2 film, and 70 for a (001) TiO_2 film.

The potentials for our calculations, both bulk and film, were formed by overlapping atomic charge densities and by using the free electron-exchange approximation with Slater exchange ($\alpha=1.0$).¹⁷ Because neutral atom-charge densities

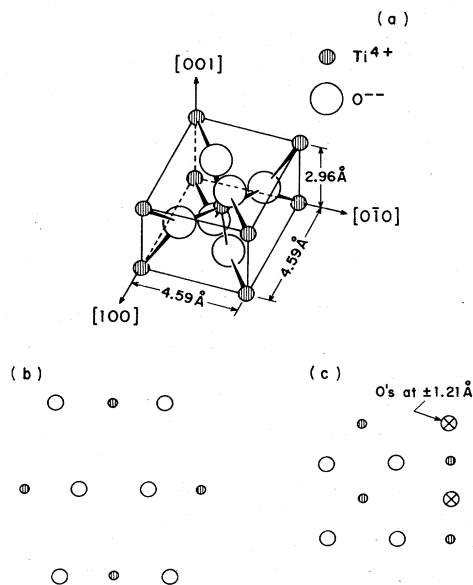


FIG. 1. (a) The TiO_2 (rutile) crystal structure. (b) View of the top layer of the TiO_2 (001) film as seen from above. (c) View of the top layer of the TiO_2 (110) film as seen from above.

lead to a band gap in excess of 5 eV even with the larger basis set, we used ionic-atomic potentials. (Madelung potentials for the superlattices were calculated using standard three-dimensional techniques).¹⁸ Using the larger basis set, we obtained a band gap of 3.0 eV (which is observed experimentally)¹⁹ only when we overlapped ionic atomic solutions of the form $Ti^{1.0+}(3d^{1.15}4s^{1.85})$ and $O^{0.5-}(2s^{2.0}2p^{4.5})$.²⁰ The unusual $3d$ occupancy was necessary as the d -band edge of the conduction band is closely related to the position of the atomic $3d$ orbital.

However, with the minimal basis set and the same ionicities used for the larger basis set, the bulk-band gap for TiO_2 increased from 3.0 to 3.6 eV although the band gap is indirect to the M point for both basis sets. To compensate for the larger band gap obtained using the minimal basis set, the atomic Ti- $3d$ occupancy was adjusted from $3d^{1.15}$ to $3d^{1.23}$ to give an indirect band gap to the M point of 3.25 eV.

Finally, the energy bands for bulk Ti_2O_3 were calculated. The atomic potentials used were $Ti^{0.75+}(3d^{1.25}4s^{2.0})$ and $O^{0.5-}(2p^{4.5})$. The $\kappa^2 = -0.4$ MTO basis set was again used.

In summary, we used a minimal MTO basis set for bulk and film calculations so that the full potential with nonspherical parts could be included. The atomic potentials were adjusted to compensate for the smaller basis set. The potentials for bulk and film were constructed according to the same prescription. All energy values were referenced to the atomic zero.⁶

The basis set simplifications used are justified since we are primarily interested in the differences between surface and bulk electronic properties. These differences can be determined because the same basis set was used for all bulk and film calculations. Finally, the reasonable agreement between calculated densities of states and observed UPS spectra for both TiO_2 and Ti_2O_3 (to be discussed later) support our contention that the minimal basis set gives a reasonably good description of our systems.

IV. ENERGY-BAND RESULTS

A. DOS for bulk TiO_2 and Ti_2O_3

The theoretical one-electron density of states (DOS) for bulk TiO_2 is given in Fig. 2, where the energy scale is referenced to atomic zero.^{6,17} All states lying below -11.0 eV are occupied while all states lying above -11.0 eV are empty. Figure 2(a) shows the total DOS while Figs. 2(b) and 2(c) show the DOS associated with the Ti and O atomic Wigner-Seitz (AWS) cells, respectively. Each DOS was obtained by broadening the energy eigen-

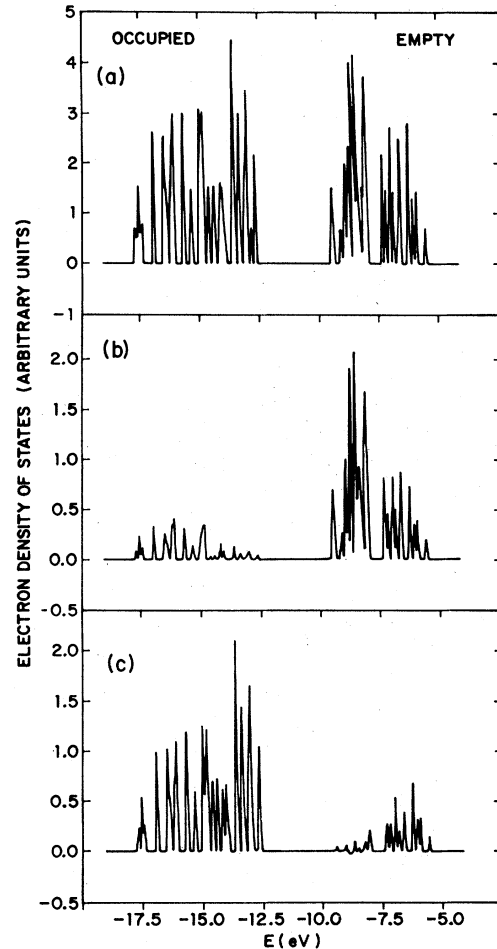


FIG. 2. Calculated one-electron density of states (DOS) for bulk TiO_2 : (a) total DOS, (b) DOS for Ti atom, (c) DOS for O atom. All levels with energies less than -11 eV are occupied and all levels with energies greater than -11 eV are empty.

values calculated at six high symmetry k points by a Gaussian of half width $\sigma = 0.002$ Ry. The DOS associated with the Ti and O sites were obtained from the probability that an electron occupies the Ti or O AWS cell. Therefore, the total DOS [Fig. 2(a)] is equal to the sum of two times the DOS of Fig. 2(b) and four times the DOS of Fig. 2(c). The conduction-band edge is at -9.24 eV and the valence-band edge is at -12.59 eV. As can be seen from Fig. 2, there is significant Ti($3d$)-O($2p$) hybridization in TiO_2 , although the valence band is predominantly O($2p$) in character and the conduction band is predominantly Ti($3d$) in character.

Comparison of the calculated density of states for bulk TiO_2 with the observed photoelectron spectrum for a TiO_2 surface shows fair agreement. In Fig. 3(b) we show the photoemission spectrum

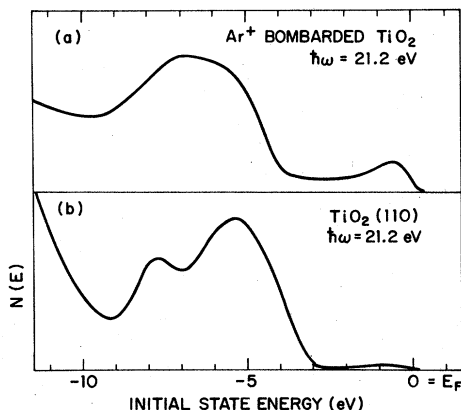


FIG. 3. Ultraviolet photoelectron spectra ($h\nu = 21.1$ eV) for (a) Ar⁺ bombarded and reduced TiO₂ (110) surface and (b) annealed TiO₂ (110) surface.

from a clean, unreconstructed TiO₂ (110) surface.⁵ (In Fig. 3 the energy scale is referenced to the Fermi energy as zero and for the sample of TiO₂ whose spectrum is shown, the Fermi energy lies just below the conduction-band edge.⁵) The experimentally observed valence-band width for TiO₂ (110) is about 6 eV and the valence band shows peaks at -5.2 and -7.7 eV. The theoretical DOS has a valence-band width of about 5.5 eV and has major groups of peaks at about -4 and -6.5 eV relative to the conduction-band edge.

In Fig. 4 we have plotted the theoretical DOS for bulk Ti₂O₃ where the energy scale is again referenced to the atomic zero.^{6,17} In this figure, all of the occupied states are crosshatched. Figure 4(a) shows the total DOS while Figs. 4(b) and 4(c) show the DOS associated with the Ti and O atomic Wigner-Seitz cells, respectively. Each DOS was obtained by broadening the energy eigenvalues calculated for four high symmetry k points with a Gaussian of half width $\sigma = 0.01$ Ry. As with TiO₂, we found that Ti₂O₃ has a gap between the predominantly O(2*p*)-derived band and the predominantly Ti(3*d*)-derived band. However, because Ti₂O₃ contains two fewer O atoms per unit cell than TiO₂, some of the Ti(3*d*) states are occupied, making Ti₂O₃ a metal rather than a wide band-gap semiconductor.

The calculated density of states for Ti₂O₃ agrees reasonably well with the observed UPS spectrum for Ti₂O₃. In Fig. 3(a) we show the UPS spectrum of heavily Ar⁺ bombarded and reduced TiO₂ (Ref. 5) (which is known to have a photoemission spectrum essentially identical to that of single-crystal Ti₂O₃).³ The experimental spectrum shows a small narrow peak at -0.7 eV (relative to the Fermi energy) and a large broad peak with a maximum at

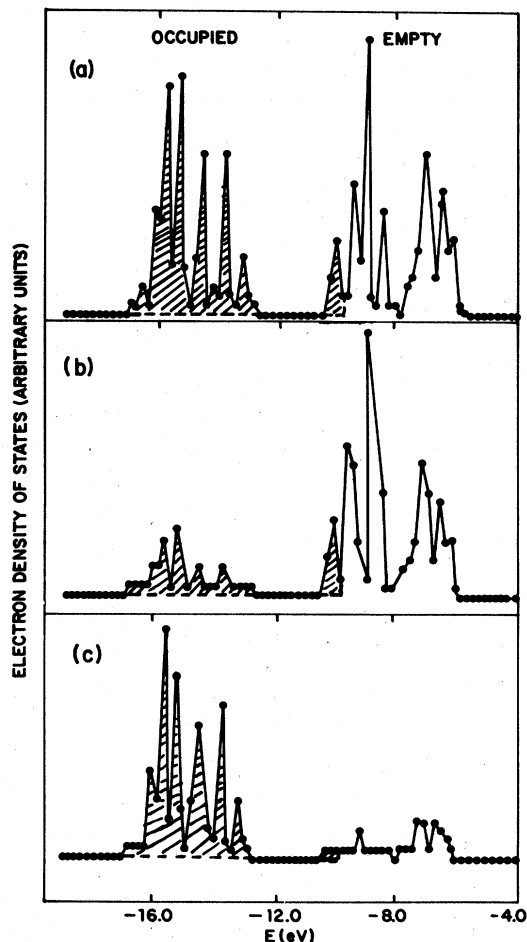


FIG. 4. Calculated one-electron density of states for bulk Ti₂O₃: (a) total DOS, (b) DOS for Ti atom and (c) DOS for O atom. All levels with energies less than -9.8 eV are occupied and all levels with energies greater than -9.8 eV are empty. The occupied levels have been crosshatched for ease of identification.

-6.8 eV. The theoretical filled DOS [see Fig. 4(a)] has the same basic structure, i.e., it has a narrow filled band near the Fermi energy which is separated by about 2.5 eV from a broader band whose peak lies at about -6 eV relative to E_F .

The most important structural difference between TiO₂ and Ti₂O₃ is the coordination of O atoms by Ti atoms, and this structural difference is reflected in the calculated densities of states, as well as in the photoemission data. The O atoms are coordinated by three Ti atoms in TiO₂ and by four Ti atoms in Ti₂O₃ while the Ti-O bond lengths and the coordination of Ti atoms by O atoms are basically the same for both materials. Therefore, it is not surprising to note that the Ti(3*d*)-derived bands for both materials [compare Figs. 2(b) and

4(b)] are quite similar in width and general structure while the O(2*p*)-derived bands [compare Figs. 2(c) and 4(c)] are substantially different in both width and general structure. Finally, we note that the trends seen in the calculated filled densities of states in going from TiO₂ to Ti₂O₃ are also seen in the photoemission data, i.e., the O(2*p*)-derived band becomes narrower, the location of the highest peak of the O(2*p*) band shifts to lower energies, and the Ti(3*d*) band becomes partially filled. This reasonable agreement between theory and experiment gives us confidence that our thin film DOS calculations will reflect the true surface behavior.

B. DOS for TiO₂ (001) film

In Fig. 5(a) we show the calculated total one-electron density of states for the unreconstructed five-layer (001) film of TiO₂, and in Figs. 5(b) through 5(d) we show the separate densities of states for the first three layers of this film. All of these densities of states were constructed by broadening the energy eigenvalues of three high-symmetry *k* points with a Gaussian of half width $\sigma = 0.01$ Ry and all energy values are again referenced to the atomic zero. The calculated band gap for this film is only 0.95 eV compared to the bulk calculated value of 3.25 eV.

Examination of the DOS presented in Fig. 5 shows that the substantial narrowing of the band gap for the (001) film is due to the presence of a large number of O(2*p*) and Ti(3*d*) surface states for this film. Comparison of the various layer DOS indicates that the large majority of both the occupied O(2*p*)-derived band-gap states (the calculated bulk valence-band-gap edge is at -12.59 eV) and the empty Ti(3*d*)-derived band-gap states (the calculated bulk conduction-band edge is at -9.24 eV) are localized in the outermost first layer, while the inner third layer has a calculated DOS more closely resembling that of bulk TiO₂. These surface states are related to Ti⁴⁺ dangling bonds present at the surface since the first layer Ti atoms are only fourfold O coordinated compared to the bulk sixfold O coordination.

We now argue that the presence of these unstructured dangling bonds on the unreconstructed (001) surface renders this surface thermodynamically unstable and their presence is thus responsible for the experimentally observed, thermally induced reconstruction, or faceting,^{4,5} of this surface. In particular, our calculations show that simple relaxation of atoms in the top layer (e.g., puckering out the O atoms in the first layer) does not substantially alter the number or location of the dangling-bond surface states. In other words, our

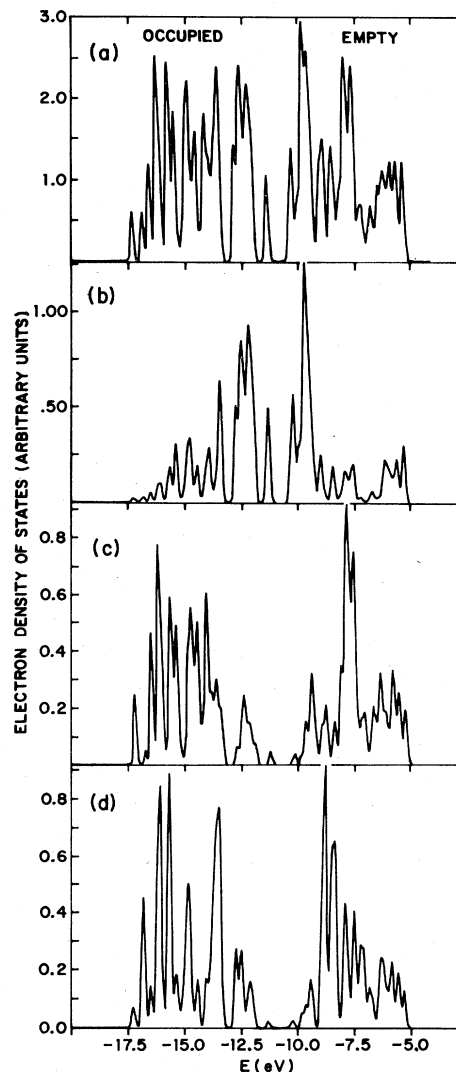


FIG. 5. Calculated one-electron density of states (DOS) for five-layer TiO₂ (001) film: (a) total DOS, (b) first layer DOS, (c) second layer DOS, and (d) third (middle) layer DOS. All levels with energies less than -11 eV are occupied and all levels with energies greater than -11 eV are empty.

calculations show that only a massive rearrangement (i.e., reconstruction or faceting) of the (001) surface leading to a substantial increase in the O coordination of the surface Ti atoms would drive the occupied band-gap surface states below the bulk valence-band edge. This observation is consistent with the observation that fourfold coordinated Ti⁴⁺ is quite rare for inorganic oxides containing titanium.²¹

C. DOS for TiO₂ (110) film

In Fig. 6 we show the total one-electron density of states for the unreconstructed and unrelaxed

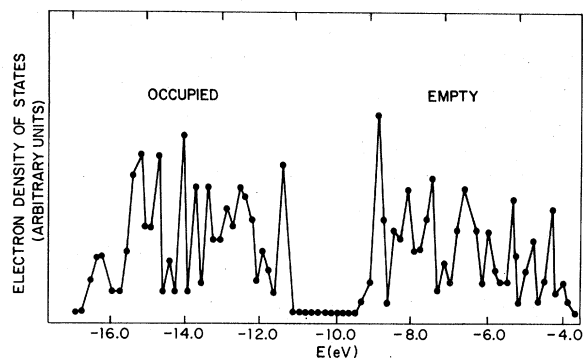


FIG. 6. Calculated one-electron density of states (DOS) for unrelaxed three-layer TiO₂ (110) film. All levels with energies less than -11 eV are occupied and all levels with energies greater than -11 eV are empty.

(110) film of TiO₂. This DOS was constructed by broadening the eigenvalues of 4 high-symmetry k points with a Gaussian of half width $\sigma = 0.01$ Ry. The energy scale was shifted +0.92 eV relative to the calculated atomic zero to account for spurious superlattice Madelung energy effects. (See the appendix for a discussion of this point and other Madelung energy considerations). The calculated band gap for this film is 1.78 eV.

Figure 6 shows that this (110) film has essentially no Ti(3d)-derived states in the band gap, but it also shows that this (110) film [like the (001) film] does have a substantial number of occupied O(2p)-derived states in the gap. However, careful examination of the one-electron potentials at various locations in the (110) film indicated that these occupied states in the gap are present because of a substantial Madelung energy effect associated with one of the surface O atoms and not because of the O coordination of Ti atoms. In Table I we list the Madelung energies at the O and Ti sites for the unrelaxed (110) film as well as the Madelung energies at the O and Ti sites of the other systems we studied. The extremely high value of the Madelung energy (-4.58 eV) for the outermost O atom in the (110) film was identified as being responsible for driving the O(2p) states into the gap. This O atom (which is bridge bonded to two Ti atoms) puckers out of the surface so that it is not surprising that its Madelung potential is substantially different from that of the other O atoms in the first layer or the O atoms in the bulk.

Since the atomic coordination is not responsible for the states in the gap, no substantial reorganization of the surface is necessary to remove them and the surface should not reconstruct. In particular, we found that if these puckered O atoms

TABLE I. Comparison of the calculated Madelung potentials at the O and Ti sites of bulk Ti^{1.0+}O₂^{0.5-}, bulk Ti₂^{0.75+}O₃^{0.5-}, five-layer (001) oriented Ti^{1.0+}O₂^{0.5-} film and three-layer (110) oriented Ti^{1.0+}O₂^{0.5-} film used in the density-of-states calculations. The energies are all given in eV. All energies are relative to the atomic zero except for the two (110) films. The Madelung energies of the unrelaxed (110) film have been shifted 0.92 eV and the Madelung energies of the relaxed (110) film have been shifted 0.50 eV to account for spurious superlattice effects (see Appendix).

Bulk TiO ₂		
Ti		11.42
O		-6.53
Bulk Ti ₂ O ₃		
Ti		8.43
O		-6.13
TiO ₂ (001) film		
First layer	Ti	10.01
	O	-5.66, -5.66
Second layer	Ti	11.77
	O	-6.76, -6.76
Third layer	Ti	11.39
	O	-6.61, -6.61
Unrelaxed TiO ₂ (110) film		
First layer	Ti	10.77, 12.03
	O	-4.58, -6.45, -6.78, -6.78
Second layer	Ti	11.52, 11.52
	O	-6.63, -6.63, -6.63, -6.63
Relaxed ($\Delta Z = 0.20$ Å) TiO ₂ (110) film		
First layer	Ti	10.56, 12.27
	O	-5.68, -6.27, -6.84, -6.92
Second layer	Ti	11.62, 11.46
	O	-6.72, -6.72, -6.55, -6.55

relax inward $\Delta Z = 0.20$ Å (changing the Ti-O bond length from 1.85 to 1.75 Å, then the Madelung potential of this puckered O atom changes -1.1 eV (see Table I), and all of the occupied band-gap states are driven below the bulk valence-band-edge at -12.59 eV. (We note here that moving O atoms in the (001) surface comparable distances alters their Madelung potentials by less than 0.2 eV.) We therefore argue that the nearly bulklike O coordination of the surface Ti atoms on the (110) surface (fivefold and sixfold on the surface compared to sixfold in the bulk) eliminates dangling bonds and leads to the thermally stable, unreconstructed surface which is observed experimentally.³⁻⁵ Finally, we note that fivefold and sixfold coordination of Ti⁴⁺ is very common in inorganic oxides containing titanium.²¹

D. Conclusions

The calculations presented here offer possible explanations for some of the observed surface properties of TiO_2 . The difference in electronic structure of different faces appears to be related to the surface O coordination of Ti. The calculated one-electron density of states of the unreconstructed (001) surface (which has only fourfold O-coordinated Ti atoms) contains a large number of filled surface states of p character within the band gap. The calculated density of states of the unreconstructed (110) surface (which has fivefold and sixfold O-coordinated Ti atoms) contains no filled surface states if the puckered O atoms relax inward by $\Delta Z = 0.20 \text{ \AA}$. Therefore, if we make the reasonable assumption that occupied surface states in the bulk band gap arise from thermodynamically unstable configurations, we are then led to the conclusion that the observed difference in stability between the unreconstructed (110) and (001) surfaces is due to their different surface electronic properties. In particular, we conclude that the free energy change associated with the removal of the dangling-bond surface states found on the unreconstructed (001) surface is expected to be the driving force for the reconstruction or faceting of this surface.

APPENDIX

It is clear from our results for the TiO_2 (110) films that for ionic (or partially ionic) materials

Madelung energy effects play a very large role in determining the calculated DOS. In this Appendix we discuss some of the details of the Madelung energy assignments we have used in our DOS calculations.

For the TiO_2 (001) film the atomic planes are all neutral and, consequently, the calculated Madelung potentials at lattice sites in the film converge rapidly to the bulk *calculated* value for film lattice sites far from the surface. In Table II we show the calculated Madelung energies at the Ti and O atom sites for both five- and seven-layer (001) oriented TiO_2 films [using the configuration $\text{Ti}^{1.0+}(3d^{1.15}4s^{1.85})$ and $\text{O}^{0.5-}(2s^{2.0}2p^{4.5})$] along with the calculated Madelung energies in bulk TiO_2 . As can be seen by the third layer of the films, the calculated Madelung potentials have converged to within 0.1 eV of the corresponding calculated values for the bulk. Also, the calculated Madelung potentials for the two different superlattice geometries (i.e., five layers vs seven layers) are equal to 0.02 eV or better.

Our observation of the rapid convergence of the calculated Madelung potentials of our superlattice model of neutral planes is consistent with the results of Wolfram *et al.*¹¹ who did an exact Madelung energy calculation for a semi-infinite set of neutral planes [(001) planes] of the partially ionic material SrTiO_3 and found a similar rapid convergence for this perovskite structure. Therefore, as a further check on our superlattice method, we did a Madelung potential calculation for a seven-

TABLE II. Calculated Madelung energies at Ti and O atom sites in bulk TiO_2 and in TiO_2 (001) films with different superlattice geometries. All energies are in eV. The ionic configurations used were $\text{Ti}^{1.0+}(3d^{1.15}4s^{1.85})$ and $\text{O}^{0.5-}(2p^{4.5})$.

Bulk TiO_2		
	Ti	11.42
	O	-6.53
Unreconstructed five-layer TiO_2 (001) film—4.33- \AA vacuum space		
First layer	Ti	10.01
	O	-5.66, -5.66
Second layer	Ti	11.77
	O	-6.76, -6.76
Third layer	Ti	11.39
	O	-6.61, -6.61
Unreconstructed seven-layer TiO_2 (001) film—4.33- \AA vacuum space		
First layer	Ti	10.01
	O	-5.67, -5.67
Second layer	Ti	11.77
	O	-6.76, -6.76
Third layer	Ti	-11.41
	O	-6.63, -6.63
Fourth layer	Ti	11.46
	O	-6.63, -6.63

layer superlattice model of an (001) surface of SrTiO₃ using the same ionicities as Wolfram *et al.*¹¹ We found that the values of the Madelung potentials calculated for the superlattice model agreed (to better than 0.1 eV) with the potentials calculated for the semi-infinite slab. This agreement led us to the conclusion that our calculated Madelung potentials for the TiO₂ (001) film were correct (to better than 0.1 eV) so that we used these values in our LCMTO calculations for this

surface.

Evaluation of the Madelung potentials for our TiO₂ (110) films was not as straightforward as it was for the TiO₂ (001) film because the charge planes making up the (110) films are non-neutral. These non-neutral planes give rise to long-range fields that extend well beyond the outer boundary of each TiO₂ slab and therefore cause interaction between the separated slabs of the superlattice. However, our Madelung energy calculations

TABLE III. Calculated Madelung energies at Ti and O atom sites for bulk TiO₂ and for TiO₂ (110) films with different superlattice geometries. All energies are in eV. The ionic configurations used were Ti^{1.0+}(3d^{1.15}4s^{1.85}) and O^{0.5-}(2p^{4.5}).

Bulk TiO ₂		
	Ti	11.42
	O	-6.53
Unrelaxed five-layer TiO ₂ (110) film—6.35-Å vacuum space		
First layer	Ti	10.10, 11.38
	O	-5.24, -7.11, -7.45, -7.45
Second layer	Ti	10.89, 10.80
	O	-7.38, -7.30, -7.28, -7.28
Third layer	Ti	10.82, 10.83
	O	-7.29, -7.29, -7.29, -7.29
Unrelaxed three-layer TiO ₂ (110) film—6.35-Å vacuum space		
First layer	Ti	9.85, 11.15
	O	-5.51, -7.37, -7.71, -7.71
Second layer	Ti	10.62, 10.52
	O	-7.64, -7.64, -7.53, -7.53
Unrelaxed five-layer TiO ₂ (110) film—12.70-Å vacuum space		
First layer	Ti	9.39, 10.71
	O	-5.72, -7.72, -8.03, -8.03
Second layer	Ti	10.19, 10.14
	O	-7.99, -7.92, -7.89, -7.89
Third layer	Ti	10.16, 10.16
	O	-7.91, -7.91, -7.91, -7.91
Unrelaxed three-layer TiO ₂ (110) film—12.70-Å vacuum space		
First layer	Ti	9.46, 10.73
	O	-5.88, -7.75, -8.09, -8.09
Second layer	Ti	10.23, 10.13
	O	-8.03, -8.03, -7.92, -7.92
Relaxed five-layer TiO ₂ (110) film—6.35-Å vacuum space		
First layer	Ti	10.18, 11.89
	O	-6.05, -6.64, -7.29, -7.29
Second layer	Ti	11.20, 11.12
	O	-7.10, -6.97, -6.95, -6.95
Third layer	Ti	11.15, 11.16
	O	-6.96, -6.96, -6.96, -6.96
Relaxed three-layer TiO ₂ (110) film—6.35-Å vacuum space		
First layer	Ti	10.06, 11.77
	O	-6.18, -6.77, -7.34, -7.42
Second layer	Ti	11.12, 10.96
	O	-7.22, -7.21, -7.05, -7.05

TABLE IV. Energy shifts required to give equivalent atomic sites in TiO_2 (110) films equivalent Madelung energies and to give the innermost atomic sites the bulk Madelung energy. All energies are in eV.

Superlattice geometry	Madelung energy shift
Unrelaxed five-layer (110) film— 6.35-Å vacuum space	0.68
Unrelaxed three-layer (110) film— 6.35-Å vacuum space	0.92
Unrelaxed five-layer (110) film— 12.70-Å vacuum space	1.32
Unrelaxed three-layer (110) film— 12.70-Å vacuum space	1.35
Relaxed five-layer (110) film— 6.35-Å vacuum space	0.37
Relaxed three-layer (110) film— 6.35-Å vacuum space	0.50

seemed to indicate that the major effect of these long-range, slab-slab interactions is to simply shift all the Madelung energies by a constant amount whose magnitude depends upon the particular superlattice geometry being used (i.e., the number of layers in the slabs and the separation between the slabs). Because exact calculations of the Madelung potentials of a semi-infinite slab of non-neutral planes have not been carried out,¹¹ our determination of the values of the Madelung potentials to use for the (110) film LCMT0 calculation was based entirely on the results of our superlattice calculations.

In Table III we list the calculated Madelung energies of the O and Ti atom sites for a number of different TiO_2 (110) superlattice geometries including both three- and five-layer films, 6.35 and 12.70-Å vacuum spacings, and relaxed and unrelaxed puckered O atoms. Examination of this table shows first that the absolute values of the Madelung potentials at equivalent sites in the films vary substantially from one superlattice geometry to another and that none of the film Madelung energies are particularly close to the bulk values. However, closer examination of the values in the table shows that the calculated energy separation

of the Madelung energies of the innermost Ti and O atom sites in the films (i.e., $\Delta E_M^{\text{film}} = 18.09 \pm 0.02$ eV for the third layer of all the five-layer films) is very close to the calculated bulk energy separation (i.e., $\Delta E_M^{\text{bulk}} = 17.95$ eV). Furthermore, if we make the constant energy shifts shown in Table IV to the Madelung energies of all of the *unrelaxed* TiO_2 (110) films, then the Madelung energies of all equivalent sites (with just one exception) agree to 0.07 eV or better, and the value of the Madelung energies of the innermost Ti and O atoms in the five-layer films agrees with the bulk values to 0.08 eV or better. In addition, with the constant energy shifts shown in Table IV for the films with relaxed puckered O atoms ($\Delta Z = 0.20$ Å), the Madelung energies of Ti and O atom sites in all but the first layer agree with the equivalent sites in the unrelaxed films to 0.01 eV or better. Based on these results, we argue that the Madelung potentials of a semi-infinite slab would have (to within 0.1 eV) the values obtained by shifting the film values by the amounts shown in Table IV. Therefore our DOS calculations for the (110) TiO_2 films were made using the shifted Madelung energies as mentioned in the text.

¹M. S. Wrighton, D. S. Ginley, P. T. Wolczanski, A. B. Ellis, D. L. Morse, and A. Linz, Proc. Nat. Acad. Sci. U.S.A. **72**, 1518 (1975).

²J. G. Mavroides, D. I. Tchermer, J. A. Kafalas, and D. F. Kolesar, Mater. Res. Bull. **10**, 1023 (1975).

³V. E. Henrich, G. Dresselhaus, and H. J. Zeiger, Phys. Rev. Lett. **36**, 1335 (1976).

⁴Y. W. Chung, W. J. Lo, and G. A. Somorjai, Surf. Sci. **64**, 588 (1977).

⁵R. H. Tait and R. V. Kasowski, Phys. Rev. B **20**, 5178 (1979).

⁶R. V. Kasowski, Phys. Rev. B **14**, 3398 (1976).

⁷O. K. Andersen and R. V. Kasowski, Phys. Rev. B **4**, 1064 (1971).

⁸E. S. Dana and W. E. Ford, *Danos Textbook of Mineralogy* (Wiley, New York, 1957).

⁹K. Vos, J. Phys. C **10**, 3917 (1977).

¹⁰J. A. Tossell, D. J. Vaughan, and K. H. Johnson, Am.

- Mineral. 59, 319 (1974).
- ¹¹T. Wolfram, E. A. Kraut, and F. J. Morin, Phys. Rev. B 7, 1677 (1973).
- ¹²G. P. Alldredge and L. Kleinman, Phys. Rev. B 10, 559 (1974); M. L. Cohen, M. Schuter, J. R. Chelikowsky, and S. G. Louie, *ibid.* 12, 5575 (1975).
- ¹³R. V. Kasowski, Phys. Rev. Lett. 30, 1175 (1973).
- ¹⁴R. V. Kasowski, Phys. Rev. B 8, 1378 (1973).
- ¹⁵R. V. Kasowski, Phys. Rev. Lett. 37, 219 (1976).
- ¹⁶Frank Herman and R. V. Kasowski, Phys. Rev. B 17, 672 (1978).
- ¹⁷F. Herman and S. Skillman, *Atomic Structure Calculations* (Prentice-Hall, Englewood Cliffs, 1963).
- ¹⁸Mario P. Tosi, Solid State Phys. 16, 1 (1964).
- ¹⁹M. Cardona and G. Harbeke, Phys. Rev. 137A, 1467 (1965).
- ²⁰This ionic configuration for Ti was suggested by L. Mattheiss (private communication).
- ²¹L. H. Brixner, J. Inorg. Chem. (U.S.S.R.) 3, 600 (1964).